Protein Science (1995), *4*:2532–2544. Cambridge University Press. Printed in the USA.

Covalent attachment of functionalized lipid bilayers to planar waveguides for measuring protein binding to biomimetic membranes[3]

STEPHAN HEYSE[1] AND HORST VOGEL[1]

[1] Institute of Physical Chemistry 4, Chemistry Department, Swiss Federal Institute of Technology, CH-1015 Lausanne, Switzerland

MICHAEL SÄNGER[2] AND HANS SIGRIST[2]

[2] Institute of Biochemistry, University of Berne, Freiestrasse 3, CH-3012 Bern, Switzerland

(RECEIVED June 13, 1995; ACCEPTED September 21, 1995)

Abstract

A new method is presented for measuring sensitively the interactions between ligands and their membrane-bound receptors in situ using integrated optics, thus avoiding the need for additional labels. Phospholipid bilayers were attached covalently to waveguides by a novel protocol, which can in principle be used with any glass-like surface. In a first step, phospholipids carrying head-group thiols were covalently immobilized onto SiO_2-TiO_2 waveguide surfaces. This was accomplished by acylation of aminated waveguides with the heterobifunctional crosslinker *N*-succinimidyl-3-maleimidopropionate, followed by the formation of thioethers between the surface-grafted maleimides and the synthetic thiolipids. The surface-attached thiolipids served as hydrophobic templates and anchors for the deposition of a complete lipid bilayer either by fusion of lipid vesicles or by lipid self-assembly from mixed lipid/detergent micelles. The step-by-step lipid bilayer formation on the waveguide surface was monitored in situ by an integrated optics technique, allowing the simultaneous determination of optical thickness and one of the two refractive indices of the adsorbed organic layers. Surface coverages of 50–60% were calculated for thiolipid layers. Subsequent deposition of POPC resulted in an overall lipid layer thickness of 45–50 Å, which corresponds to the thickness of a fluid bilayer membrane.

Specific recognition reactions occurring at cell membrane surfaces were modeled by the incorporation of lipid-anchored receptor molecules into the supported bilayer membranes. (1) The outer POPC layer was doped with biotinylated phosphatidylethanolamine. Subsequent specific binding of streptavidin was optically monitored. (2) A lipopeptide was incorporated in the outer POPC monolayer. Membrane binding of monoclonal antibodies, which were directed against the peptide moiety of the lipopeptide, was optically detected. The specific antibody binding correlated well with the lipopeptide concentration in the outer monolayer.

Keywords: antibody; integrated optics; lipopeptide; membrane receptor; planar waveguide; supported lipid bilayer; thiolipid

Reprint requests to: Horst Vogel, DC-ICP 4, EPFL, CH-1015 Lausanne, Switzerland; e-mail: horst.vogel@icp.dc.epfl.ch.

Abbreviations: APTES, γ-aminopropyl-triethoxysilane; biotin-DPPE, *N*-((6-(biotinoyl)amino)-hexanoyl)-1,2-dipalmitoyl-*sn*-glycero-3-phosphoethanolamine; DMF, dimethylformamide; DMPC, 1,2-dimyristoyl-*sn*-glycero-3-phosphocholine; DMPSH, 1,2-dimyristoyl-*sn*-glycero-3-phosphothioethanol; DOPSH, 1,2-dioleoyl-*sn*-glycero-3-phosphothioethanol; DTNB, 5,5′-dithio-bis-(2-nitro-benzenic acid); IgG, immunoglobulin G; IOS, integrated optical scanner; NANP, peptide sequence Asn-Ala-Asn-Pro; OG, *N*-octyl-β-D-glucopyranoside; POPC, 1-palmitoyl-2-oleoyl-*sn*-glycero-3-phosphocholine; SMP, *N*-succinimidyl 3-maleimidopropionate; SPR, surface plasmon resonance.

[3] The major part of the work was performed at the Swiss Federal Institute of Technology, partly to fulfill a Ph.D. thesis (SH). Waveguide modifications were performed at the University of Berne (MS and HS).

Many biologically important signal transduction processes occur at the level of cell membranes via specialized membrane receptors (Shinitzky, 1995). Prominent examples are neuroreceptors such as ligand-gated ion channels (Unwin, 1993), G-protein-coupled receptors (Strader, 1994), and immunoglobulin receptors (Ravetch & Kinet, 1991). For the understanding of the molecular mechanisms of such processes, it is important to investigate the respective ligand-receptor events either directly in vivo or in an artificial, reconstituted membrane system (McConnell et al., 1986; Thompson et al., 1993). In the case of channel proteins, extremely sensitive techniques have been developed to observe the opening and closing steps of single channels formed by receptor proteins by measuring electrical conductance changes

using patch-clamp or planar lipid bilayer techniques (Rudy & Iverson, 1992). However, in many other cases, no direct changes of the electrical membrane properties are involved during the receptor-ligand interactions, as for example with G-protein-coupled receptors. In order to investigate such events on a molecular level, radioactive or fluorescent labels have been introduced for distinguishing the molecular events involved by a combination of rather complicated and time-consuming experimental procedures (Feder et al., 1986; Heithier et al., 1992).

Here we present a new method for investigation of the interactions between ligands and membrane receptors directly, without the need for additional labels, yet with high sensitivity. A lipid bilayer, comprising membrane-bound receptor molecules, is covalently attached to the suitably functionalized surface of an optical transducer. We used TiO_2/SiO_2 waveguide layers with an incorporated input grating coupler, which register refractive index changes caused by deposition of lipid layers and the binding of ligands with sufficiently high molar mass to the supported membrane (Fig. 1). In contrast to surface plasmon resonance sensors for label-free measurement, the waveguide technique allows two optical parameters to be measured simultaneously, of which adlayer thickness and refractive index values can be derived. It can be easily combined with other spectroscopic or fluorescence techniques due to the absence of an absorbing metal layer (Zhou et al., 1991). The grating coupler employed in the present study is an example of an easy-to-handle integrated optical sensor, which was introduced as an analytical tool by Tiefenthaler and Lukosz (1989). Covalent linkage between the lipid bilayer and the solid support offers mechanically stable, long-lasting, and regenerable membranes that may also have important practical applications for the development of a new class of biosensors using membrane protein receptors as the biologically selective recognition element.

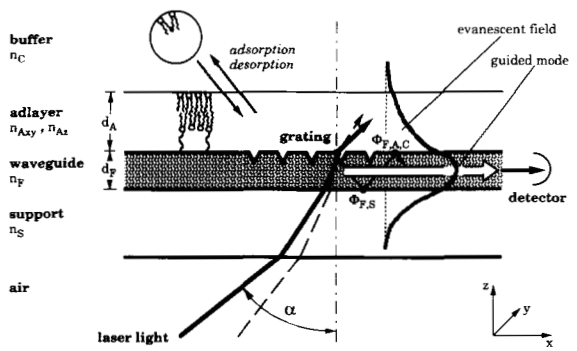

Fig. 1. Configuration for waveguide measurements, not drawn to scale. Shown is a section through a waveguiding film with embossed diffraction grating fixed on a glass support. On the waveguide surface, lipid molecules are bound, forming an adlayer. Laser light comes from below under varying angles of incidence α (depicted are two light rays). The solid line represents a light ray that meets the incoupling condition; the light is coupled into the waveguide by the grating and is guided to the detector ("guided mode"). Schematically depicted is the field of the guided mode, which decays exponentially into adlayer and buffer media ("evanescent field"). For illustrative reasons, the zigzag ray picture with phase shifts $\Phi_{F,A,C}$ and $\Phi_{F,S}$ at the interfaces is also included, although it is not really valid for monomode waveguides. Light with a different angle of incidence (dashed line) is not coupled into the waveguide. During a measurement, the angle of incidence α is continuously changed while measuring the intensity of the guided modes. The presence of an organic adlayer modifies the evanescent field and the incoupling angle changes with respect to the bare waveguide. From this angle shift, the thickness d_A and one of the refractive indices n_{Axy} or n_{Az} of an anisotropic organic adlayer are derived. For these calculations, the refractive indices of buffer n_C, waveguiding film n_F, and glass support n_S, as well as the waveguide thickness d_F, have to be known.

Strategies for the covalent attachment of lipid layers on optical devices have been already realized in the case of gold surfaces for SPR measurements using disulfide-bearing phospholipids (Lang et al., 1992, 1994) and disulfide-functionalized amphiphilic copolymers (Erdelen et al., 1994).

Unlike the gold surfaces of SPR sensors, the thin waveguide layers used in the present work consist of hydrophilic glass-like materials with high refractive indices (e.g., Ta_2O_5, TiO_2, TiO_2/SiO_2-mixtures), to which covalent attachment of lipids is not possible without functionalization of either the support or the lipid molecules, or both. The new approach presented here is conceptually simple. It entails, firstly, the modification of the hydroxylated waveguide surface with an aminosilane; secondly, the reaction of the surface amino functionalities with a heterobifunctional, maleimide-carrying crosslinker; and, finally, the immobilization of synthetic thiolipids. By this procedure, covalent bonds are formed between thiol functions at the lipid head groups and the thiol-reactive maleimido groups on the waveguide surface. This highly selective reaction is performed in aqueous environment under mild conditions, with no byproduct. In a final step, the surface-attached thiolipids serve as templates and anchors for the formation of a complete lipid bilayer by vesicle fusion or by self-assembly from mixed lipid-detergent micelles. This procedure is simple, fast, and reproducible. Thiolipids with a polar spacer between phosphate and sulfur group allow for a further decoupling of the lipid layer from the solid support and provide an aqueous environment on both sides of the bilayer that is sufficiently large to accommodate the extramembranous parts of a membrane-traversing protein; this concept was realized previously on gold surfaces (Lang et al., 1992, 1993, 1994). Although chemical crosslinkers have been used for tethering thiol-bearing proteins and oligonucleotides to various supports (Hong et al., 1994; Lee et al., 1994), to our knowledge, no attempts have been made so far to anchor lipid bilayers to hydrophilic supports using maleimide chemistry.

The feasibility of the new method for the formation of surface-anchored membranes and their utility for studying reactions at membrane surfaces is demonstrated by three examples (Fig. 2). Firstly, pure lipid membranes are assembled on the sensor surface in order to characterize the new method of membrane formation and detection in detail. Secondly, biotinylated lipids, incorporated in the supported membrane, act as simple membrane receptors for the study of specific recognition reactions occurring at membrane surfaces, in this case the binding of streptavidin to the biotinylated lipid. This ligand–receptor interaction has been investigated in detail on other interfaces elsewhere (Weber et al., 1989; Häussling et al., 1991; Reiter et al., 1993; Spinke et al., 1993). It served in this study as standard for ligand binding to the newly developed membrane system. Finally, lipopeptides with a threefold repeat of the amino acid sequence Asn-Ala-Asn-Pro (NANP in one-letter code) as the peptide moiety are incorporated into the supported membranes in order to detect the specific binding of an anti-$(NANP)_n$-antibody to its lipid-anchored peptide antigen. The NANP sequence was chosen because of its clinical relevance for the im-

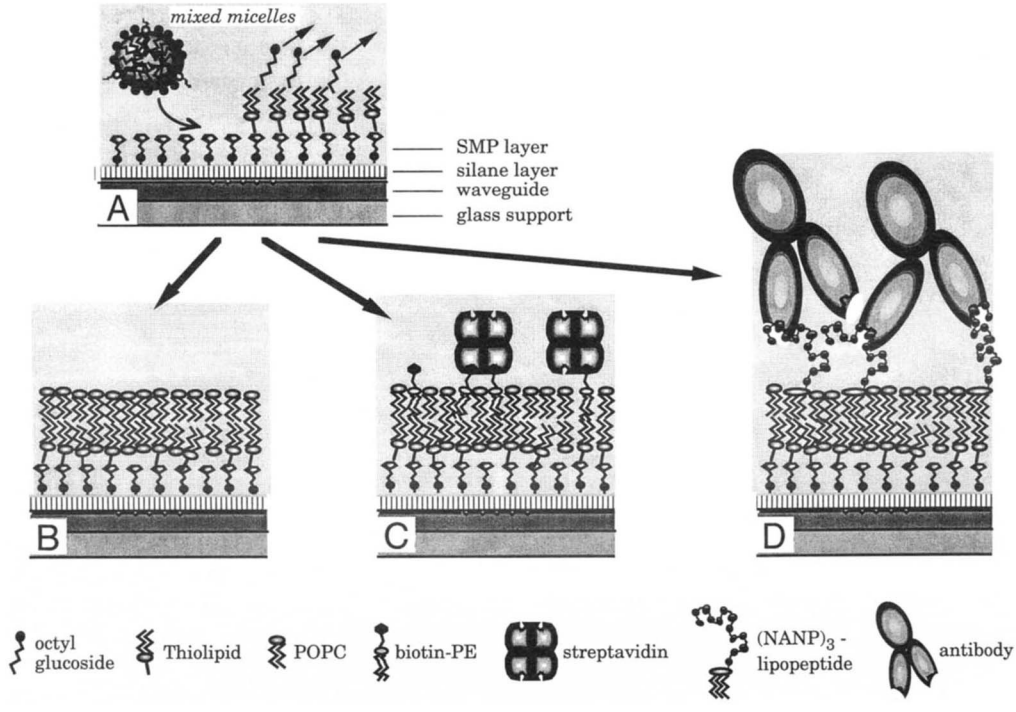

Fig. 2. Schematic representation of the three different supported lipid bilayer systems studied in this work. **A:** Binding of thiolipids from mixed micelles to a maleimide-modified waveguide surface and subsequent removal of detergent by washing with buffer. This anchor layer was then completed to give a lipid bilayer in different ways. **B:** Self-assembly of phospholipids onto a thiolipid layer from vesicles or mixed micelles established a bilayer linked to the waveguide surface. Note that phospholipids also formed part of the lower bilayer leaflet, because the thiolipid layer was not compact. **C:** Self-assembly of phospholipid vesicles containing a fraction of biotinylated lipids lead to a functionalized membrane, to which streptavidin bound. **D:** Self-assembly of a phospholipid/$(NANP)_3$-lipopeptide mixture from an OG mixed micellar solution formed a bilayer containing lipid-anchored peptide antigens. Specific and nonspecific binding of a monoclonal anti-$(NANP)_n$ antibody to this membrane were investigated.

mune response against malaria parasites.[4] In addition, SPR experiments were performed with correspondingly functionalized, supported lipid membranes on gold surfaces, and compared with those on the integrated optics device. A detailed description of the antibody-$(NANP)_n$ surface reactions using SPR will be published elsewhere (Duschl et al., 1995).

Results

Functionalization of waveguide surfaces with maleimides

A prerequisite for the covalent anchoring of thiolipids to the optical waveguide is a two-step chemical modification of the surface as outlined in Figure 3: (1) silanization of the waveguide with APTES, resulting in waveguide surface **A** with surface-exposed amino groups; (2) derivatization of amino groups with SMP, resulting in waveguide surface **B** with exposed maleimide groups at the surface.

Prior to silanization, waveguides were subjected to basic and acidic oxidative etching, which resulted in an increase of surface exposed hydroxyl groups, the reaction partners of the silane. Liquid-phase silanization of etched sensor chips in toluene resulted in approximately 1.6 nmol NH_2/cm^2 on the sensor chip surface, comprising the waveguide layer and the glass support. This corresponds to an average of 10 accessible NH_2 groups/nm^2 on surface **A**, assuming that the waveguide and the glass support are silanized to the same extent. Additional ellipsometry measurements showed that a silane layer about 5 Å thick was deposited on a silicon wafer with this silanization protocol (data not shown).

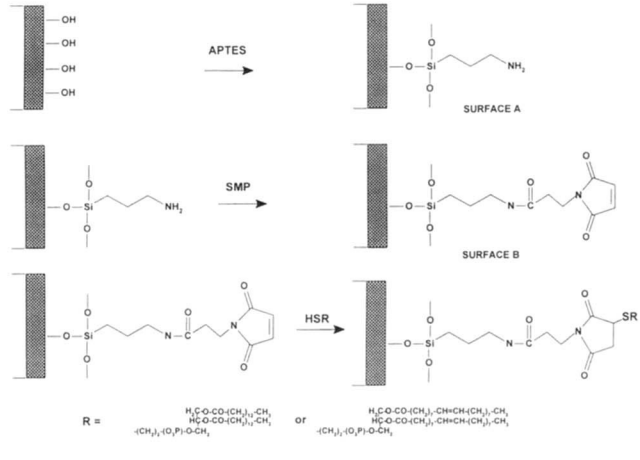

Fig. 3. Scheme of waveguide surface modification.

[4] A tandom repeat of the NANP sequence represents the major antigenic part of the circumsporozoite (CS) protein of human malaria parasites, *Plasmodium falciparum*. This protein uniformly surrounds the parasite as a coat (Godson, 1985). The concentration of anti-CS antibodies in the blood of patients is a reliable indicator for malaria infection. Fast and sensitive test methods such as the presented integrated optics technique are of practical importance in medical diagnostics and also in vaccine development, because anti-CS antibodies protect against the parasite in vivo and in vitro (Romero et al., 1989).

The selective binding of sulfur-containing molecules to waveguide surface **B** was documented using [^{35}S]-cysteine. Modification of waveguides **A** with SMP resulted in a 15-fold increase in cysteine binding compared to unspecific cysteine adsorption on unmodified waveguides **A**. Preincubation with β-mercaptoethanol abolished the specific cysteine binding to waveguides **B**. The surface density of specifically bound cysteine and thereby of the maleimide functionalities could not be determined exactly, because the specific activity of the [^{35}S]-cysteine was only broadly specified by the supplier (20–150 mCi/mmol). Due to this uncertainty, a density of about 90–700 pmol bound cysteine per cm^2 waveguide **B** was estimated, corresponding to 0.5–4 molecules per nm^2. If the thiolipids would bind with identical efficiency as cysteine, there would be 0.25–2 lipid binding sites on the surface per 50 Å^2, the area of a thiolipid molecule.

Thiolipid binding to waveguide surface B

The covalent attachment of thiolipids to waveguide surfaces **B** was performed in aqueous media, thus enabling optical monitoring of layer formation in situ. Lipids were solubilized in the form of small micelles with the head-group thiols accessible from the aqueous phase, in order to make the formation of thioethers with the immobilized maleimides possible (Fig. 3). Due to the high critical micellar concentration of the detergent OG (approximately 20 mM at 20 °C), it could be easily removed from the resulting thiolipid layer by washing with buffer. Figure 4 shows a typical optical measurement of membrane formation on waveguide surfaces **B** and subsequent protein binding.

Both DOPSH and DMPSH formed layers of similar mean thickness of about 13 and 11 Å, respectively (Table 1). The self-assembly of either thiolipid on modified waveguides was complete (>95%) after 30–60 min. Thiolipid binding changed the optical anisotropy of the system. The refractive index in the *x-y* plane (n_{Axy}) had to be set higher with respect to the index perpendicular to the surface (n_{Az}) in order to obtain identical lipid layer thickness values from both waveguide modes. This yielded values of $\gamma > 1$ (Table 1).

The covalent attachment of the thiolipid layer was proven by the following observations. (1) Thiolipid layers formed from mixed micelle solutions on waveguide surfaces **B** were insensitive to detergent washing. However, they could be completely removed by a single OG wash step if the surface maleimide groups had been inactivated by previous exposure to mercaptoethanol. (2) The binding of radiolabeled cysteine was 6–7-fold lower on thiolipid-covered than on untreated waveguide surfaces **B**. Preincubation of waveguides **B** with DMPC/OG mixtures did not result in an inhibition of subsequent cysteine binding, which demonstrates the stability of maleimides toward OG and the specificity of thiolipid binding.

Thiolipid binding to waveguide surfaces **B** increased the hydrophobicity of the surface as shown by high water contact angles on the thiolipid surface ($\theta \approx 90°$).

The sensor chips often showed a drift of the effective waveguide indices N_{TE} and N_{TM} after changing the cover medium or altering the ionic strength (e.g., buffer change). This effect was reported to be reduced by soaking the sensor chips overnight in the buffer solution used later for the experiments (Ramsden & Schneider, 1993). But for the study of thiolipid binding, this strategy could not be applied because waveguide surfaces **B** lost up to one third of their cysteine-binding capacity when stored overnight at 4 °C in buffer B, probably due to maleimide decomposition (Kitagawa et al., 1981). Therefore, thiolipid binding was performed immediately after maleimide modification of aminated waveguides. To evaluate the amount of thiolipid bound to the surface, the drift underlying the measured binding signals was modeled as described below (see Waveguide theory and data processing) and subtracted from the experimental data (Fig. 5).

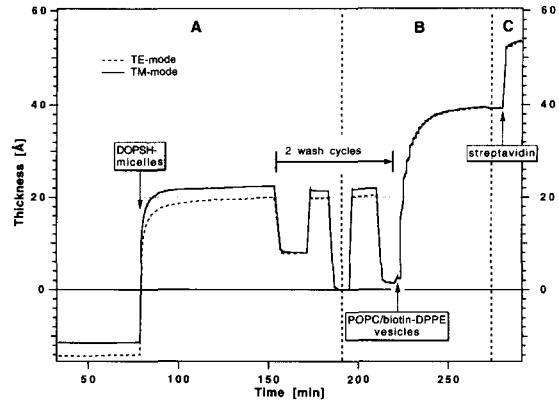

Fig. 4. Formation of a lipid bilayer on a maleimide-modified waveguide followed by streptavidin binding. Shown are the apparent thickness values of the waveguide adlayer versus time, calculated with Equation 3 from the experimentally determined effective waveguide indices N (Equation 1) with $n_{Axy} = n_{Az}$. The waveguide surface was washed once with OG at the beginning of the experiment (not shown). Both waveguide modes were evaluated separately to give thickness values for the adsorbed layers. **A:** The first layer consisted of DOPSH thiolipid. It was added to the activated surface in the form of OG mixed micelles. This resulted in adsorption to the waveguide that produces part of the increase in the measured signal. After 15–60 min, a steady state was reached. Noncovalently bound lipids were removed by washing consecutively two times with buffer, OG solution, and buffer again. Most of the apparent thickness increase on thiolipid addition is due only to the refractive index change when replacing buffer by the detergent-solubilized thiolipid. The actual average thickness of the thiolipid layer bound to the surface is evaluated as the difference between the signal of the buffer before adding "DOPSH micelles" and the measured stable signal of the thiolipid layer after the second washing step. This value was arbitrarily defined as 0 Å on the thickness axis. As a consequence, the measurement, starts at negative values. In this measurement, the two polarizations of the laser light (*TE*- and *TM*-modes) yield different thickness values for the isotropically calculated thiolipid layer. This can only be explained by the assumption that the thiolipid binding changes the overall anisotropy of the system. **B:** Self-assembly of the second layer from POPC vesicles doped with 2 mol% biotin-DPPE. **C:** After rinsing with buffer, streptavidin solution was added.

On gold surfaces, adsorption of DOPSH resulted in a mean layer thickness of 21 Å, as measured by surface plasmon resonance. This is about twice the value obtained for binding to maleimide-modified waveguides. The time course of binding, however, was similar. On gold, the self-assembly of DOPSH was complete after 60 min.

Formation of a supported lipid bilayer

The upper leaflet of the supported bilayer represents the reactive membrane surface, e.g., for the interaction of membrane-bound receptors with their ligands in the aqueous environment. The bilayer was completed exclusively by self-assembly techniques, starting from lipid vesicles or lipid-detergent micelles, which contained a certain fraction of receptor molecules, where needed. Examples for the formation of supported lipid bilay-

Table 1. *Characterization of lipid layers on modified waveguide surfaces by integrated optics and on gold by surface plasmon resonance*

No.	Thiolipid[a]	Phospholipid[a] (method)	Thickness [Å][b]	Anisotropy coefficient[c]	Number of experiments
Lipid layers on maleimide-modified waveguides					
1	**DOPSH**	–	13 ± 5 (11 ± 2)	1.023 ± 0.01	8 (3)
2	**DMPSH**	–	11 ± 1	–	2 (0)
3	DOPSH	**POPC** (vesicles)	28 ± 7 (29 ± 9)	0.990 ± 0.004	9 (5)
4	DOPSH	**POPC** (micelles)	30 ± 5	0.995 ± 0.002	3 (3)
5	DMPSH	**POPC** (micelles)	31 ± 5 (28 ± 2)	0.993 ± 0.001	3 (2)
6	DOPSH	**POPC/2% biotin** (vesicles)	36 ± 4 (35 ± 5)	0.996 ± 0.003	6 (5)
7	DMPSH	**POPC/2% LP** (micelles)	27 ± 5 (23 ± 5)[d]	1.001 ± 0.001	4 (2)
8	DMPSH DOPSH	**POPC/0.5-4% LP** (micelles)	31 ± 5	–	9 (0)
9	**DOPSH**	**POPC** (vesicles)	47 ± 8 (47)	–	4 (1)
Lipid layers on gold surfaces					
10	**DOPSH**	–	21 ± 7	–	4
11	DOPSH	**POPC** (vesicles)	24 ± 10	–	3
12	**DOPSH**	**POPC** (vesicles)	46 ± 13	–	3
Three typical experiments on maleimide-modified waveguides (bilayer formation by vesicle fusion to DOPSH template)					
13	**DOPSH**	**POPC**	21 + 27	–	–
14	**DOPSH**	**POPC**	9 + 39	1.029/0.993	–
15	**DOPSH**	**POPC/2% biotin**	11 + 39	1.012/0.995	–

[a] Lipid bilayers were produced by first binding thiolipid to waveguides **B** from mixed micelle solutions and subsequently assembling phospholipids or mixtures of phospholipids either with biotinylated lipids or with lipopeptides, by the method indicated in brackets. LP stands for $(NANP)_3$-lipopeptide.

[b] Mean average thickness values given here refer to the lipid layers indicated in bold letters, i.e., to incomplete mono- or complete bilayers. They were calculated using an index of refraction of $n_{Az} = 1.45$. Results given in parentheses were from measurements with stable, nondrifting sensor chips only.

[c] The anisotropy coefficient is $\gamma = n_{Axy}/n_{Az}$. It refers to the lipid layer indicated in bold letters. It was determined only for these chips that showed a stable optical signal.

[d] In the case of membranes formed on DMPSH with a mixture of POPC/2% lipopeptide, some experiments gave smaller values, which lowered the mean value to $d_A \approx 27$ Å. However, in order to make precise measurements without drift, the waveguide chips had to be incubated overnight with the thiolipid micellar solution and so the packing of the thiolipid base layer was not known.

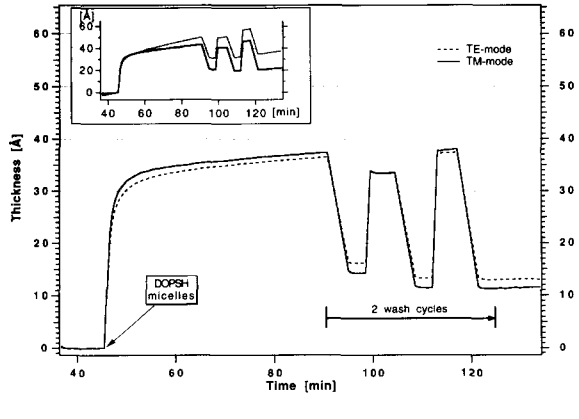

Fig. 5. Binding of the DOPSH thiolipid to the maleimide-modified waveguide. The curves were obtained by subtracting the baseline drift from the measurement shown in the inset. Original data of the inset were obtained as described in Figure 4. After 47 min incubation of the sensor chip in buffer, a DOPSH micellar solution (1 mg/mL lipid in 50 mM OG) was applied for 45 min. It was then exchanged for buffer and washed twice with OG solution and buffer (98–122 min). Due to the elevated index of refraction of the detergent solution, these washing steps appear as peaks.

ers with incorporated biotinylated lipids or lipopeptides are shown in Figures 4B and 6A, respectively. Vesicles of different composition adsorbed to the thiolipid surfaces always with an exponential-like time course. The mean thickness for pure POPC and mixed POPC/lipopeptide layers self-assembled on thiolipid layers ranged from 27–31 Å both for vesicle and mixed micelle techniques (Table 1). Optical measurements indicated that the supported bilayers were stable in buffer and did not desorb upon alteration of the ionic strength. By washing with OG, the second layer was entirely removed. It could be reconstructed by vesicle fusion or micelle dilution. Thus, the thiolipid-modified chips were reusable, as far as lipid layer formation is concerned. Supported layers containing conventional and biotinylated lipids showed distinctly higher thickness values of 36 Å.

Comparative experiments were performed on thiolipid-covered gold surfaces. POPC vesicles adsorbed quickly to these surfaces and formed stable layers within 30–60 min, as judged by surface plasmon resonance. They were approximately 24 Å thick, which is distinctly thinner than those assembled on thiolipid-modified waveguide surfaces.

However, when the thickness values of covalently bound thiolipid and subsequently self-assembled lipid layers are added, the

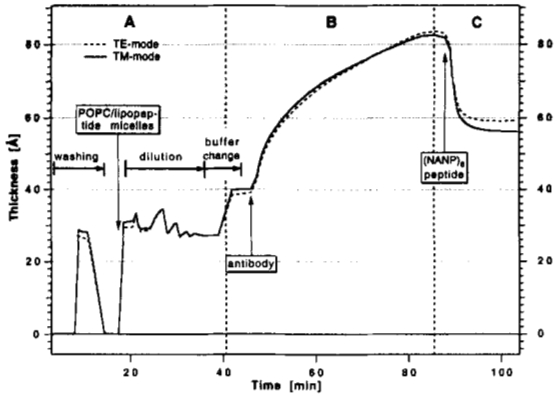

Fig. 6. Antibody binding to a lipid membrane containing $(NANP)_3$-lipopeptide. The waveguide was incubated with DOPSH and then left in detergent solution overnight to reduce drift effects. **A:** After one washing step with OG (7–15 min), a second lipid layer was formed by applying a 50 mM OG solution containing 1.24 mM POPC and 0.027 mM lipopeptide (=2 mol%) and subsequent dilution 10 times 1:1 (v/v) with buffer. **B:** The buffer was exchanged for antibody buffer, causing a change in the index of refraction of the medium, which caused a jump in the measured signal. Then a solution of 200 nM antibody was added (t = 47 min), resulting in a continuous binding reaction. **C:** After washing with buffer, part of this antibody was finally displaced upon addition of 75 μM free antigen $(NANP)_6$. Thickness values were calculated isotropically with n_A = 1.45, as described in Figure 4. The antibody binding and desorption reactions were evaluated using the refractive index of the antibody buffer for the cover medium index.

sum lies between 45 and 50 Å, for experiments on waveguide surfaces and on gold surfaces. For example, the three experiments listed in Table 1 (lines 13–15) show that, on a surface covered by a 20-Å thiolipid layer, subsequent lipid vesicle adsorption yielded an additional 30-Å layer, whereas on a 10-Å base layer, the POPC layer was about 40 Å thick. This indicates that a less densely packed thiolipid first layer may be filled up on adsorption of POPC to give a final thickness of about 50 Å. Such calculations could, of course, only be performed for those experiments where both the thiolipid binding and the subsequent bilayer assembly were monitored independently.

During formation of the second layer, the optical anisotropy changed to give a lower in-plane refractive index n_{Axy} (n_{Az} was kept constant all the time). This yielded values of $\gamma < 1$ (Table 1). Notable exceptions were layers containing lipopeptides, which seemed not to change the overall anisotropy (Fig. 6A; Table 1). We noted that the initial thiolipid binding usually changed the anisotropy of the system in the opposite direction.

Streptavidin binding to a biotin-functionalized supported lipid membrane

The well-established streptavidin–biotin system was used as our first model for the functionalization of self-assembled membranes with receptor sites and the subsequent specific binding of protein from solution.

Streptavidin bound to a supported biotin-containing membrane with two phase kinetics: a fast phase, during which the main part of the binding occurred, followed after 3–5 min by a slow increase in effective waveguide index (Fig. 4C). To evaluate the data quantitatively, thickness values at t = 500 s after streptavidin injection were chosen as reference for all measurements. This gives a mean thickness of the protein layer of 16 ± 3 Å (n_A = 1.45; the same refractive index was taken for the protein as for the lipid layers). After t = 500 s, the thickness of the streptavidin layer still increased slowly, up to 15% within 1 h. Because the amount of bound protein was independent of the streptavidin concentration between 0.4 and 1.7 μM, we conclude that the streptavidin concentration was not the limiting factor for binding.

To measure nonspecific binding, streptavidin was added to POPC/thiolipid-supported membranes not containing biotin. In these experiments, less than 1 Å increase of mean layer thickness was observed. Similarly, low nonspecific binding was observed when exposing membranes formed from biotin-DPPE-containing vesicles to complexed streptavidin (i.e., streptavidin whose binding sites had been previously blocked by incubation with soluble biotin).

Antibody binding to a supported lipid membrane containing $(NANP)_3$-lipopeptide

As a more complex model system for ligand–receptor interactions, we incorporated $(NANP)_3$-lipopeptide into supported membranes and measured the binding of anti-$(NANP)_n$ antibodies to the functionalized membrane surface.

Upon addition of antibody, a high mass adsorption on the membrane was observed (Fig. 6B). It proceeded much more slowly than the streptavidin binding to biotin-containing membranes described above. The total mass adsorption depended on the lipopeptide content of the membrane-forming mixed micelle solution (Fig. 7). In the absence of lipopeptide (pure POPC second layer), the amount of nonspecifically bound antibody corresponded to a protein layer with an average thickness of 5–7 Å. With increasing lipopeptide content, more antibody adsorbed. This was most pronounced in the region between 0.5 and 2% lipopeptide, then leveling off. At 0.5% lipopeptide/99.5%

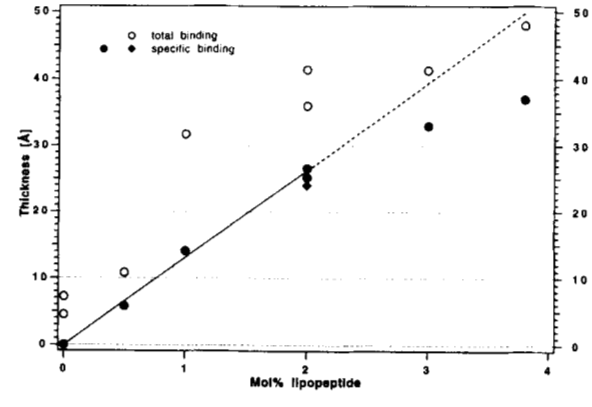

Fig. 7. Binding of anti-$(NANP)_n$ antibodies to $(NANP)_3$-lipopeptide-doped POPC membranes on thiolipid surfaces. Shown are the thickness values of the antibodies bound versus the ratio lipopeptide/total lipid in the mixed micelle solution used for the formation of the supported bilayer. Total binding (○) corresponds to the increase in the apparent thickness (n_A = 1.45) of the adlayer observed upon addition of the 200 nM antibody solution. Specific binding (●) designates the amount of protein that is desorbed after addition of 75 μM $(NANP)_6$ peptide. The specific binding of antibodies to a mixed layer on an alkylated gold surface is also shown (◆). The dotted line is the linear regression of the values for specific binding up to 2 mol% lipopeptide.

POPC, the adsorbed antibody layer was approximately 10 Å thick; at 2% lipopeptide/98% POPC, it was 40 Å thick.

After antibody binding, free $(NANP)_6$ antigen in high concentration (75 μM) was added. This led to a partial desorption of the protein from the surface (Fig. 6C). The $(NANP)_6$ concentration had been chosen such that it assured maximal antibody desorption. The amount of protein that could be desorbed increased linearly up to 2 mol% lipopeptide in the membrane (Fig. 7). On raising further the lipopeptide:POPC ratio, this "specific binding" increased more slowly, and was now proportional to the total binding of antibody to the membrane. The difference between the amount of antibody that bound and the amount that could be subsequently desorbed corresponded to a 10-Å thick layer of nonspecifically bound protein. Control experiments showed that free $(NANP)_6$ peptide bound to a membrane doped with 2% lipopeptide and produced a layer of about 1 Å mean thickness. When the binding of antibody and subsequent desorption by free $(NANP)_6$ were repeated on the same supported membrane, the following results were obtained. The quantity of antibody binding in the second cycle equaled the amount that had been desorbed from the membrane by addition of free $(NANP)_6$ in the first cycle. The addition of $(NANP)_6$ in the second cycle caused desorption of almost the same amount of antibody (90%) as in the first cycle.

The results obtained were, within experimental error, identical for both DMPSH and DOPSH anchoring lipids.

In experiments with surface plasmon resonance on gold surfaces, two kinds of self-assembled layers were used to form the first leaflet of the membrane:DMPSH thiolipid layers and tetradecanethiol layers. On DMPSH/POPC layers, prepared by micelle dilution, nonspecific binding of anti-$(NANP)_n$ antibodies occurred, corresponding to a 10-Å protein layer. Such adsorbed antibodies were not desorbed upon $(NANP)_6$ addition. In contrast, pure POPC layers prepared on an alkylthiol surface did not show any nonspecific binding of anti-$(NANP)_n$ antibodies. Nonspecific binding was not observed, either, when mixed POPC/lipopeptide layers on alkylthiols were exposed to nonspecific IgG.

When lipopeptide-containing supported layers on alkylthiol surfaces were exposed to anti-$(NANP)_n$ antibodies, a high mass adsorption was observed. On a membrane containing 2% lipopeptide, it amounted to a 24-Å protein layer (Fig. 7). This is in the same range as the specific antibody binding in the corresponding experiments on waveguides. In contrast to the results on waveguides, virtually all bound material could be subsequently desorbed within a few minutes by addition of free $(NANP)_6$. Furthermore, the thiol layer could be perfectly regenerated by removing the POPC/lipopeptide membrane with OG.

Discussion

In the present concept, lipid bilayers are anchored via covalently attached thiolipids to waveguide surfaces. The method yields imperfect, covalently bound thiolipid layers that can be converted to lipid bilayers by self-assembly of phospholipids. Receptor molecules are easily incorporated into these layers. An integrated optics technique allows to monitor layer formation and binding of ligands in real time.

As anchor molecules, thiolipids were chosen, in order to produce similar lipid membrane systems on hydrophilic waveguides to those produced on gold by Lang et al. (1994). DMPSH and DOPSH form self-assembled monolayers on gold surfaces. This enabled us to investigate the layer formation with surface plasmon resonance and to compare structural aspects of chemisorbed thiolipid layers with thiolipid layers covalently attached by maleimide chemistry to planar waveguides.

The ASI 2400 monomode waveguide chips were chosen as substrate for our supported membranes for three reasons: their commercial availability, their high sensitivity, and the waveguide material (SiO_2/TiO_2 mixture). This oxide surface offers an alternative to the gold surfaces used for surface plasmon resonance and it seemed well-suited for modification with the surface chemistry established on silica surfaces. However, in the progress of this work, the drift of most of the waveguides had to be coped with, which required a fitting procedure and which rendered the monitoring of SMP binding to aminopropylated waveguides as well as all long-term measurements impossible. We suppose that the scattering of our data might be linked to this drift and to the observed variation in chip quality. Nellen and Lukosz (1993) have proposed an improved procedure for manufacturing more reproducible sensor chips with reduced waveguide drift, but the development of improved waveguides was beyond the scope of this work.

Thiolipid immobilization via maleimides

Surface derivatization of TiO_2/SiO_2 waveguides with primary amines is required for maleimide grafting. Many different protocols varying in the deposition method, reaction time, temperature, and solvents have been described for the amination of hydroxylated surfaces with APTES (Vandenberg et al., 1991). Uncatalyzed liquid-phase deposition in refluxing toluene was used in our study for the silanization of sensor chips. A similar protocol was used by Kallury et al. (1989) for the silanization of oxidized silicon wafers, which were subsequently used as substrates for the covalent immobilization of phospholipids in a "head-out" orientation.

Here, maleimide surface grafting was performed by reacting the succinimide ester of SMP with primary amines on the waveguide surface, resulting in the formation of an amide bond. Binding of radiolabeled cysteine served as a tool to demonstrate the presence and thiol-selectivity of waveguide-grafted maleimides. Retention of covalently immobilized cysteine upon prolonged sonication in aqueous media provides evidence for the stable linkage of the maleimide-terminated silane layer to the waveguide. With our modification scheme, thiolipids are covalently bound to waveguide surfaces **B**. This is evident from the stability of the thiolipid layer against detergent washing and from competitive cysteine-binding assays.

Choice of refractive index for optical measurements

The effective refractive indices N_{TE}, N_{TM} measured during the different binding reactions can be transformed into an optical thickness $\Delta n^x d_A$ of the lipid and protein adlayer (Δn is the difference in refractive index between the organic film and the surrounding medium, d_A is the geometrical thickness of the organic film). The optical thickness is directly related to the adsorbed mass on the waveguide and thereby to the number of adsorbed molecules.

To convert the optical into a geometrical thickness, a refractive index has to be assumed. Calculated with constant refractive index, the "adlayer thickness" becomes a measure of molecule density; only at close packing it can be interpreted in terms of molecular dimensions. According to published data obtained with well-defined model systems, $n = 1.45$ is a reasonable value for the refractive index of lipids in a fluid state and adsorbed proteins (Lang et al., 1992, 1994; Spinke et al., 1992, 1993; Reiter et al., 1993; Terrettaz et al., 1993) (and references therein).[5] For lipids and fatty acid salts in a crystalline state, refractive indices in the range of $n = 1.5$ seem more appropriate (Swalen, 1986; Kooyman & Krull, 1991; Schmidt et al., 1992). But in our experiments, a crystalline state of lipids on the waveguide can be excluded (see below).

Optical measurements of thiolipid layers

To obtain reference data for the thiolipid layers on waveguides, a series of surface plasmon resonance measurements of thiolipid immobilization on gold surfaces were performed. On gold surfaces, the hydrocarbon chains of gold-attached alkylthiols and thiolipids pack as closely as possible in a nearly hexagonal manner (Fenter et al., 1994; Lang et al., 1994). In the case of DOPSH, we determined optically a thickness of 21 Å. X-ray diffraction analysis yielded a transmembrane distance of 44 Å between the choline groups of a DOPC bilayer (Wiener & White, 1992). Lang et al. (1994) determined a monolayer thickness of 22–27 Å ($n = 1.45$) for a different thiolipid with a longer spacer than DOPSH and with saturated palmitoyl chains. Therefore, we conclude that the experimentally obtained value of 21 Å in our case corresponds to a monolayer of DOPSH.

Thiolipid layers formed on waveguides reached a stable limiting structure after 30–60 min. However, they turned out to be incompletely packed monolayers, because the corresponding mass adsorption was only 50–60% of that on gold surfaces. These data suggest that, on average, only half of the geometric waveguide surface was covered by thiolipids. A mean layer thickness of 11 Å was found also by ellipsometry measurements on oxidized silicium wafers that were subjected to the same treatment as the waveguides (result not shown). Accordingly, the incomplete surface coverage of the thiolipid must be a result of the coupling chemistry, implying either (1) a submonolayer coverage of the crosslinker; (2) an inefficient binding of thiolipids to close-packed maleimide groups; (3) maleimide decomposition preceding exposure to thiolipid; or (4) a combination of these reasons. In principle, the incompleteness of the anchoring layer is an advantage for future incorporation of membrane-spanning proteins.

Bilayer formation

There is evidence for the formation of a lipid bilayer when a thiolipid-modified waveguide surface is exposed either to lipid vesicles or to mixed micelles that are subsequently diluted. The resulting layer composed of thiolipids and conventional phospholipids had always an identical thickness of about 47 Å, despite variations in thiolipid coverage. Therefore, it is assumed that adsorbing phospholipids fill up "holes" in the first thiolipid leaflet. Interestingly, DOPSH/POPC bilayers on gold surfaces show essentially the same thickness of about 46 Å. It was shown by capacitance measurements (unpubl.) that, in this case, too, the adsorbing phospholipids seemed to fill up "holes," because the layer capacitance approached a bilayer value during adsorption. The lipid film thickness of 47 Å on modified waveguides is in the same range as published data on DOPC bilayers (44 Å, Wiener & White, 1992), fluid DMPC bilayers adsorbed on quartz (43 Å, Johnson et al., 1991), and mixed POPC/thiolipid layers on gold (47 Å when using $n = 1.45$, Lang et al., 1994). Furthermore, in the latter publication, the authors performed a POPC assembly experiment on incomplete thiolipid layers, which yielded finally a similarly structured membrane to the POPC assembly on dense thiolipid base layers, as judged from electrical data (Lang et al., 1994). In summary, these experimental results lead to the conclusion that lipid bilayers were established on the waveguide surfaces.

With both DOPSH and DMPSH as template, and with either self-assembly method for POPC, the same thickness of the supported bilayer was attained. According to calorimetric and film balance measurements (data not shown), a densely packed layer of DMPSH, which contains saturated hydrocarbon chains, should be in the ordered state at 20 °C, whereas DOPSH should be in the disordered state. Obviously, the different lipid chain structure did not imply a different adsorption behavior. This is a good indication that the SMP crosslinker acts as a flexible linker, decoupling the thiolipid-anchored lipid bilayer from the solid support similarly as reported by Lang et al. (1994) for the case of gold supports. The supported bilayer shows optical anisotropy ($n_{Az} \neq n_{Axy}$), which has previously only been observed for crystalline Langmuir-Blodgett films of single-chain amphiphiles (Ulman, 1991).

For biotin-containing vesicles, we recorded a higher mass deposition (36 Å) on thiolipid surfaces than with pure POPC vesicles (28 Å). This difference cannot be accounted for by the slightly different masses of POPC and biotin-DPPE. Literature data on thickness of supported DMPC and DPPC monolayers doped with 5 mol% biotin-DPPE range from 16 Å (Spinke et al., 1992) to 31 Å (Schmidt et al., 1992) at $n = 1.50$ (corresponding to 23 Å or 44 Å, respectively, evaluated at $n = 1.45$). So far, we cannot give an experimentally validated reason for our layers being thicker when prepared from vesicles doped with biotin-DPPE.

The lipopeptide layers produced by the micelle dilution technique were in the same thickness range as POPC layers. It seems, therefore, justified to conclude that the membranes obtained were stable bilayers. The theoretical increase of adsorbed mass compared to a pure POPC layer would be about 4% for a membrane containing 4 mol% lipopeptide. This would cause an increase in layer thickness of 1 Å, which is below the detection limit, given the scatter in our data.

Protein binding to functionalized membranes

The applicability of the integrated optics technique for investigation of specific recognition reactions on membrane surfaces

[5] Stenberg et al. (1991) used a different method of calibration, correlating SPR angle shifts with the amount of adsorbed radiolabeled protein. Nevertheless, a generalization of this calibration relies on the assumption that the refractive index of the protein under investigation corresponds to that of the standard proteins used for the calibration. We calculated the refractive indices of mixed systems composed of proteins in buffer with the Bruggemann effective medium approximation (Aspnes, 1982), which showed that a refractive index of $n = 1.47$ for proteins would describe the angle shifts observed by Stenberg et al.

was demonstrated by Ramsden and Schneider (1993). They studied the binding of antibodies to a glycolipid-anchored protein attached to a phospholipid membrane. These authors prepared a lipid bilayer on the waveguide surface by a two-step Langmuir-Blodgett transfer of lipid monolayers from the air-water interface. Unlike our self-assembly process, this procedure is not suitable for the integration of transmembrane proteins and is not designed for repeated use of the sensor chip.

Here we have investigated protein binding to the supported membranes, first with the biotin-streptavidin binding reaction, which is a well established test system (Weber et al., 1989; Häussling et al., 1991; Reiter et al., 1993; Spinke et al., 1993). The major part of the binding of streptavidin to layers containing biotin was instantaneous, followed by a slow process. Similar two-phase kinetics were also observed by Reiter et al. (1993) for streptavidin binding to a biotin-functionalized monolayer at the air-water interface and were explained by a lateral rearrangement of bound streptavidin molecules. Furthermore, these authors found that the binding of streptavidin strongly depends on the structure of the lipid monolayer, being highest in the fluid-expanded and gas-analogue states. Our data point to a fluid state of the outer leaflet of the supported membrane, with the biotin residues presented in a well-accessible and laterally mobile form. The amount of adsorbed streptavidin indicates that all biotinylated lipids are involved in the binding of streptavidin.

To avoid steric packing problems, the biotin/POPC ratio in the vesicle solution was chosen below the ratio needed for binding of a complete streptavidin monolayer to a supported membrane. At 2 mol% biotin in the membrane-forming vesicle solution, our measurements yield 16 Å as protein layer thickness after 500 s incubation. Assuming a linear dependence between binding and the receptor site density below 5 mol%, our results are consistent with Spinke et al. (1992), who found 41 Å for the streptavidin layer bound to a membrane doped with 5 mol% biotin on a polymer support. Taking the structural data of Darst et al. (1991) for 2D crystals of streptavidin at the air-water interface (lateral dimensions of one streptavidin molecule 55×45 Å^2, thickness 50 Å), one gets an expected average thickness of the protein layer on a lipid layer containing 2 mol% biotin of 20 Å, if each streptavidin molecule binds two biotin molecules. Streptavidin binding to mixed layers corresponds well to the expected value, additionally indicating that the actual composition of the layers corresponds well to that of the vesicle dispersion.

On layers containing lipopeptide, bound antibodies that could be desorbed by addition of free $(NANP)_6$ were considered specifically bound, whereas the remaining fraction was considered nonspecifically bound. This evaluation method was validated by the following experiments. (1) On gold surfaces, antibody bound to pure lipid membranes of POPC on thiolipid templates could not be desorbed by $(NANP)_6$. (2) Using mixed POPC/2 mol% lipopeptide layers on alkylthiols, all bound antibody could be desorbed. (3) On waveguides, the same amount of antibody was removed by $(NANP)_6$ from mixed layers of the same composition, but this time formed on thiolipid templates, in spite of some antibody remaining unspecifically bound.

Nonspecific antibody binding to supported membranes on waveguides becomes more prominent with increasing lipopeptide content of the membrane, indicating a disturbing effect of the lipopeptide on the membrane structure.

Specific antibody binding to the membrane correlates linearly up to 2 mol% with the lipopeptide concentration in the membrane-forming micelle solution. Modeling the antibodies as spheres, a densely packed protein layer with an average thickness of 47 Å is obtained at 2.8 mol% lipopeptide, assuming that every antibody binds two lipopeptides and all lipopeptides are involved. At 2 mol% lipopeptide, the layer of bound antibodies would be 33 Å thick. The actual lipopeptide concentration in the supported membrane may, of course, not be 2 mol%. However, the linear dependence of the specific antibody binding on the lipopeptide content of the mixed micelle solution (up to 2 mol%) shows that it is possible to control the amount of membrane-incorporated lipopeptide.

On densely packed alkylated gold surfaces, antibodies bound to lipopeptide-containing layers were completely displaced upon addition of free antigen. Additionally, nonspecific antibody adsorption was negligible on pure POPC layers lacking lipopeptides formed upon alkylthiols. Therefore, we conclude that, on alkylthiol templates on gold, a perfectly closed outer lipid layer can be formed that blocks completely unspecific protein binding. A similar effect was observed for cholera toxin and phosphatidylcholine layers (Terrettaz et al., 1993). Nonspecific antibody binding to supported lipid bilayers on waveguides must at least partly be attributed to the particular thiolipid used. One reason might be the short ethyl spacer between headgroup phosphate and sulfur of the thiolipids, which might not permit the formation of a well-ordered first bilayer leaflet. The defects in the supporting layer may propagate to the outer leaflet, resulting in unshielded hydrophobic regions, onto which antibodies readily adsorb. The observation that nonspecific antibody binding is lower on POPC/thiolipid membranes coupled via aminopropylsilane and crosslinker to the waveguide surface than on membranes directly bound to gold via the thiolipid's thiol group indicates the importance of a flexible spacer for formation of the template layer.

Conclusions

Functionalized lipid bilayers anchored by covalently bound thiolipids have been established on waveguides by self-assembly processes in aqueous media. The coupling scheme is simple and works under mild conditions, yielding a very stable thiolipid layer of 50–60% surface coverage. Phospholipid self-assembly, starting from vesicles or micelles, converts this layer to a lipid bilayer. With our coupling scheme, the membrane is kept at a distance from the surface, thus maintaining a certain membrane flexibility and allowing for an aqueous phase between surface and bilayer. Mixtures of phospholipids and functionalized lipids or lipid-anchored peptides in different mixing ratios can be applied, yielding a functionalized membrane surface of variable composition. Membrane formation and recognition reactions at the membrane surface can be monitored optically in real time, with high sensitivity and without the need for labels. Two optical parameters of the membrane system, one of its refractive indices and its thickness, were determined independently, thus allowing a detailed characterization.

Specific and nonspecific binding of antibodies to a lipopeptide-containing membrane could be discriminated. It turned out that the lipid bilayer not only serves as a matrix for the incorporation of membrane-anchored receptors, but simultaneously reduces the nonspecific binding of proteins, such as antibodies.

This property of lipid membrane surfaces has been adopted for the development of biocompatible materials (Chapman, 1993) and might also be useful for sensor surfaces (Lang et al., 1993, 1994; Terrettaz et al., 1993). The remaining nonspecific binding of protein to supported membranes on sensor surfaces might be further reduced using thiolipids with long hydrophilic spacer groups for the template layer or using lipids presenting flexible chains of oligoethoxides or sugar moieties at the outer membrane surface. The use of lipid-anchored NANP peptides for the detection of anti-NANP antibodies by label-free optical techniques represents a new principle of immunosensors, here applicable for the diagnosis of malaria and in vaccine development.[4]

The coupling scheme is applicable to hydroxyl-exposing surfaces in general, so it could, for example, also be applied to the modification of glass surfaces to form supported bilayers. Such substrates would be suited for the fluorescence detection of specially labelled ligands at membranes (Wise & Wingard, 1991; Zhou et al., 1991). Fluorescence techniques would offer a superior sensitivity, giving detection of single molecules (Eigen & Rigler, 1994; Nie et al., 1994); however, the inherent disadvantage is the necessity of labels. The detection limit of label-free integrated optics measurements is much higher, but the sensitivity of the method presented can certainly be increased by improving the chemical stability of the waveguide material and thus reducing drift effects.

The concept of lipid immobilization is designed to allow the incorporation of transmembrane proteins in their active state into supported lipid bilayers. These proteins require aqueous phases on both sides of the membrane and a minimal membrane fluidity. Immobilized membranes have great potential for the development of new biosensors and the study of reconstituted biological signal cascades, which mostly involve transmembrane proteins and protein–protein interactions at the membrane surface (Lang et al., 1993).

Materials and methods

Materials

1,2-Dioleoyl-*sn*-glycero-3-phosphothioethanol (DOPSH); 1,2-Dimyristoyl-*sn*-glycero-3-phosphothioethanol (DMPSH) and 1-palmitoyl-2-oleoyl-*sn*-glycero-3-phosphocholine (POPC) were purchased from Avanti Polar Lipids, Alabaster/Alabama (USA). 1,2-Dimyristoyl-*sn*-glycero-3-phosphocholine (DMPC) was supplied by Sigma. *N*-((6-(biotinoyl)amino)-hexanoyl)-1,2-dipalmitoyl-*sn*-glycero-3-phosphoethanolamine (Biotin-DPPE) was from Molecular Probes, Eugene/Oregon (USA). The synthetic lipopeptide *N*-palmitoyl-S-[2,3-bis(palmitoyloxy)-(2RS)-propyl]-[R]-cysteinyl-[S]-seryl-$(NANP)_3$ (further termed "lipopeptide") was kindly provided by the group of G. Jung, Institut für organische Chemie, Universität Tübingen, Germany. It had been synthesized according to a procedure described elsewhere (Metzger et al., 1991). Tetradecanethiol was obtained from Fluka in purum quality. Monoclonal anti-$(NANP)_n$-antibody Sp3E9 raised against a $(NANP)_{40}$ peptide was a generous gift of Dr. H. Matile, Hoffmann-La Roche AG, Basel, Switzerland. The antibody was 95% pure (SDS-PAGE). Streptavidin was purchased from Boehringer Mannheim AG, in BioChemika quality. The synthetic peptide $C(NANP)_6Y$, "$(NANP)$,"[6] was synthesized by Dr. Anne Sévin, using a solid-phase strategy and Fmoc protection (Atherton et al., 1979). *N*-octyl-β-D-glucopyranoside (OG) was either from Sigma or Bachem AG, Bubendorf/Switzerland. *N*-succinimidyl 3-maleimidopropionate (SMP) was supplied by Fluka. [^{35}S]-cysteine (specified activity range 20–150 mCi/mmol) was from Amersham. (Aminopropyl)triethoxysilane (APTES) was obtained from Merck and purified by distillation under vacuum. All other chemicals used were reagent grade. The water used was purified via an ion exchanger purification train (Nanopure D4752 system, Barnstead) with attached 0.2-μm filter (Supor, DCF specification). The buffers used were: 25 mM sodium phosphate buffer, pH 8.0 (buffer A); 25 mM sodium phosphate buffer, pH 6.8 (buffer B); 66 mM sodium phosphate buffer, pH 7.0, with 100 mM NaCl added (Ab-buffer) for antibody binding experiments.

Waveguide instrumentation

Planar optical waveguides incorporating an embossed grating with grating period $\Lambda = 1/2{,}400$ mm were obtained from ASI AG, Zürich, Switzerland (type 2400, ca. 170 nm TiO_2:SiO_2 2:1 waveguiding layer of refractive index $n_F \approx 1.8$ on AF 45 glass substrate of refractive index $n_S \approx 1.52$). These sensor chips were measured with the Integrated Optics Scanner IOS-1 from ASI. The conditions for chemical surface modification were optimized using waveguides made from the same material as the sensor chips but lacking the grating coupler. A custom-made open cuvette was used to hold the reaction solution (200–400 μL) placed on top of the grating coupler of the optical waveguide.

Silanization of waveguides with APTES

Prior to silanization, sensor chips (4.8 × 1.6 cm) were cleaned by first incubating them for 5 min in a hot (90 °C) 1:1:5 mixture of $NH_4/H_2O_2/H_2O$, followed by rinsing three times with double-distilled water. The chips were then treated for 5 min with a hot 1:1:5 mixture of $HCl/H_2O_2/H_2O$, again washed extensively with double-distilled water, then rinsed three times with acetone before being vacuum dried for 12 h. The overall optical quality of the sensor chips was not affected by this treatment, although it resulted in a decrease in the waveguide thickness of about 5% of its initial value, as determined by measuring the waveguide parameter d_F with the grating coupler against air before and after etching (two sensor chips measured).

Silanization was performed by incubating at 120 °C for 3 h a single chip in 30 mL of dry toluene containing 0.5 mL (2.15 mmol) of APTES. The solvent was removed at the end of the reaction, and the chip was washed with chloroform (five times), acetone (twice), and methanol (five times). Finally, the chip was dried under a stream of nitrogen and kept in acetonitrile at 4 °C until use. The number of NH_2 groups per sensor surface area (TiO_2/SiO_2 waveguide layer and glass support) after silanization was determined with ninhydrine as described by Sarin et al. (1981).

Modification of aminated waveguides with SMP

Silanized sensor chips were removed from acetonitrile, dried under a stream of nitrogen, and stored in buffer A for at least 12 h. The sensor chips were then placed between two tight-fitting metal plates, the grating area on the waveguide surface being accessible by a circular teflon-lined 1.5 cm^2 opening in the cover metal plate. After washing twice with buffer A, the amino-

silane layer on the waveguide was treated with 200 μL of a 25 mM solution of the heterobifunctional crosslinker SMP in buffer A/DMF 4:1 (v/v). After incubation for 30 min at ambient temperature, excess reagent was removed by washing once with DMF and 10 times with buffer B.

[^{35}S]-Cysteine binding assays

Maleimide-functionalized areas on waveguides, kept between two metal plates as described above, were covered immediately after SMP modification with 100 μL of a solution of [^{35}S]-cysteine in buffer B (0.1 μCi/μL). After incubation for 1 h at ambient temperature, excess radioactive cysteine was removed by rinsing 10 times with buffer B. The sensor chip was then removed from the metal plates and the modified area was cut out (1.6 × 1.8 cm). The sample was sonicated for 30 s in buffer B and then washed abundantly with the same buffer. Retained radioactivity was measured by subjecting the sample to liquid scintillation in toluene/Triton X-100/2,5-diphenyloxazole/1,4-Bis-2-(5-phenyloxazolyl)benzene on a K-3000 scintillation counter from Kontron. Controls for the specific binding of cysteine to maleimide functionalized waveguides were carried out as described above by applying [^{35}S]-cysteine to etched or aminated waveguides, or to maleimide-functionalized waveguides that had been inactivated with β-mercaptoethanol (10% in buffer B [v/v]) prior to incubation with [^{35}S]-cysteine.

Real-time monitoring of thiolipid binding to the waveguide

Thiolipid/OG mixed micelle solutions were prepared by dissolving a dried thiolipid film (0.5 mg) in 500 μL of a 50 mM solution of OG in buffer B. The presence of thiols in the dispersion was assayed by the development of yellow color after 1:1 mixing with Ellman reagent (10 mM DTNB in water, Riddles et al., 1983). Immediately after modification with SMP, the waveguide chip was assembled with the open O-ring cuvette and mounted on the turntable of the Integrated Optics Scanner (IOS). The waveguide/cuvette assembly was rinsed twice with buffer B, then the baseline of the waveguide was recorded. The buffer was exchanged for the mixed micelle solution and the thiolipid binding was monitored with the IOS. After different times of incubation (ranging from 30 min to 16 h) at ambient temperature, the waveguide surface was rinsed with buffer B. Physisorbed lipid was removed by washing with 50 mM OG.

Formation of the lipid bilayer and protein binding

After thiolipid binding to the waveguides, lipid bilayers of POPC, of POPC/biotin-DPPE, or of POPC/lipopeptide in selected molar ratios were formed by vesicle spreading (Kalb et al., 1992; Lang et al., 1992, 1994; Terrettaz et al., 1993) or by dilution of mixed micelle solutions (Lang et al., 1994). Vesicle dispersions were produced by first drying down a chloroform solution of 1 mg either of POPC or a mixture of POPC and biotin-DPPE. After addition of 50 μL buffer B to the lipid film, the aqueous mixture was sonicated 3–4 times for 3 min in a bath-type sonicator (Sonorex RK 102p) until a clear vesicle dispersion was obtained. This dispersion was diluted to a final lipid concentration of 1 mg/mL. Two-hundred microliters of a vesicle dispersion were placed on the grating region of the thiolipid-modified waveguide and the lipid adsorption was measured until a stable layer was obtained. Excess vesicles were then removed without disturbing the formed layer by diluting 1:1 (v/v) with buffer B 10 times, while continuously maintaining the waveguide covered with buffer.

For experiments with lipopeptide, dilution of mixed micelle solutions was used exclusively for producing the second layer on top of the thiolipid layer. POPC dissolved in chloroform or mixtures of POPC and lipopeptide dissolved in chloroform: methanol 1:1 (v/v), were dried and subsequently dissolved in 50 mM OG solution in buffer B (final concentration 1 mg/mL lipid). Two-hundred microliters of this solution were placed on the thiolipid-modified waveguide. After 5 min, dilution was started by adding 200 μL buffer, mixing, and removing 200 μL of the sample. This procedure was repeated 10 times, allowing the sample to equilibrate between the dilution cycles for at least 1.5 min.

Streptavidin binding to POPC membranes with or without incorporated biotin-DPPE was measured by injecting a solution of streptavidin in buffer B into the cuvette volume, to give final concentrations of 0.4–1.7 μM streptavidin. Binding was allowed to take place for 5–45 min, and unbound protein was removed from the reaction solution by dilution (10 times 1:1 with buffer B).

Antibody binding to POPC membranes containing 0–4 mol% lipopeptide was initiated by injecting a solution of 0.3 mg/mL Anti-$(NANP)_n$ antibody in Ab-buffer to give final antibody concentrations of 100–200 nM. The binding was allowed to continue for 15–40 min, then unbound antibodies were removed by washing with Ab-buffer.

Specifically bound antibodies were displaced from the membrane surface by adding 66 μL of a 0.6 mg/mL $(NANP)_6$ solution in Ab-buffer (final $(NANP)_6$ concentration 75 μM).

Waveguide theory and data processing

The waveguides were read out by varying the angle of incidence, α, of laser light onto the grating while measuring the intensity of the guided modes (Fig. 1). This angle scan is automatically performed by the IOS, yielding the incoupling angles (at maximal intensity of guided light reaching the detectors) for the two polarizations of the light, transverse electric, *TE*, and transverse magnetic, *TM*. These angles α_{TE} and α_{TM} are directly related to the effective waveguide indices N_{TE} and N_{TM}, i.e., the ratio of the vacuum velocity of light to its velocity along the waveguide, by the incoupling condition (Tiefenthaler & Lukosz, 1989). It is written here for the first grating order and in the positive direction:

$$N = n_{air} \cdot \sin \alpha + \frac{\lambda}{\Lambda}. \quad (1)$$

n_{air} is the refractive index of air, α the incoupling angle in air, λ the vacuum wavelength of the laser light (632.8 nm), and Λ the grating period (1/2,400 mm).

From a theoretical point of view, light is coupled into a slab waveguide only if the transverse resonance condition is fulfilled (Kogelnik, 1979), i.e., the sum of all phase shifts on a path across the waveguide and back equals to a multiple m of 2π.

This is expressed in the mode equation (Tiefenthaler & Lukosz, 1989; Spohn, 1994):

$$2k_{z,F}d_F + \Phi_{F,S} + \Phi_{F,C} = m \cdot 2\pi, \tag{2}$$

where $k_{z,F}$ is the perpendicular wave vector component of the wave guided in the film F, d_F the thickness of the film (the product $k_{z,F}d_F$ is the phase shift upon traversing the waveguide), and $\phi_{F,S}$ and $\phi_{F,C}$ are the phase shifts upon total internal reflection at the interfaces, waveguiding film F/substrate S, and film F/cover medium C, respectively. These phase shifts are different for the two polarizations of the light.

Because the refractive indices of substrate, n_S, and cover medium, n_C, are both smaller than N, the field in these media is evanescent. This evanescent wave traveling along the waveguide surface is modified by the presence of an organic layer on top of the waveguide. This adlayer changes the values of $k_{z,F}$ and the phase shifts $\phi_{F,A,C}$, and thus tunes the resonance to new effective indices N. An extensive treatment of this "four-layer planar waveguide model" is given elsewhere (Tiefenthaler & Lukosz, 1989). It consists of the glass support (index **S**), the waveguiding film (**F**), the organic adlayer (**A**), and the cover medium (**C**), with the corresponding parameters: thickness **d**, refractive index **n**, effective waveguide index **N**. We calculated thickness values $\boldsymbol{d_A}$ for the organic adlayer from the effective waveguide indices $\boldsymbol{N_{TE}}$ and $\boldsymbol{N_{TM}}$ provided by the IOS with the following formulae, derived from the mode equation and the Fresnel equations:

$$d_A = \frac{1}{2|k_{z,A}|} \ln\left(\frac{k_{z,A}/n_A^{2\rho} - k_{z,C}/n_C^{2\rho}}{k_{z,A}/n_A^{2\rho} + k_{z,C}/n_C^{2\rho}} \cdot \frac{1-a}{1+a}\right). \tag{3}$$

$\boldsymbol{k} = 2\pi/\lambda$ is the wavevector of the light, $\boldsymbol{k_z}$ its component in the z-direction (perpendicular to the waveguide) given by:

$$k_{z,X} = \sqrt{n_X^2 - N^2}, \tag{3a}$$

where the index X is F, S, C, or A.

$$a = \left(\frac{n_A}{n_F}\right)^{2\rho} \cdot \frac{k_{z,F}}{|k_{z,A}|} \times \tan\left[m\pi - k_{z,F}d_F - \arctan\left(\left(\frac{n_S}{n_F}\right)^{2\rho} \cdot \frac{|k_{z,S}|}{k_{z,F}}\right)\right]. \tag{3b}$$

The coefficient $\boldsymbol{\rho}$ is set to zero for the *TE*-mode, to 1 for the *TM*-mode.

Because refractive index n_F and film thickness d_F varied from chip to chip, a waveguide calibration had to be done individually for each chip. The waveguide—usually already chemically modified—was first measured in buffer B. n_F and d_F values, which served as references for the determination of subsequently formed adlayers, were calculated assuming a three-layer model (with substrate, waveguide, and cover medium as the layers).

Lipid mono- and bilayers may show an optical anisotropy (Swalen, 1986). Under these circumstances, three parameters have to be determined for the adlayer: its refractive index in the membrane plane, n_{Axy}; the index perpendicular to the plane, n_{Az}; and its thickness, d_A, versus two measured parameters, N_{TE} and N_{TM}. We proceeded in the following way. For n_{Az}, we assumed a constant value of 1.45, which is a reasonable value for fluid lipid membranes and proteins (Pethig, 1979). Then, the second refractive index, n_{Axy}, and the mean layer thickness, d_A, were calculated numerically by setting $d_A(TE) = d_A(TM)$. From the effective waveguide index changes for the two modes upon lipid binding, two parameters were finally derived: the corresponding layer thickness, d_A, and the anisotropy coefficient, γ, which gives the ratio of the two refractive indices n_{Axy}/n_{Az} of the anisotropic layer. The thickness values $d_A(TE)$, $d_A(TM)$, calculated with the isotropic assumption $n_{Axy} = n_{Az} = 1.45$, were used to give an estimate of the error, because some of our measurements reflect anisotropy of the waveguide itself and thus the two measured parameters N_{TE}, N_{TM} may not be completely independent (Spohn, 1994).

To evaluate experiments for waveguides showing drift of the waveguide indices N, the following approach was used. During an experiment, the waveguide was exposed several times to buffer B only, without any reaction taking place. The changes of the optical properties of the waveguide observed during these time intervals can be formally described by an apparent change in the adlayer thickness d_A'. The values d_A' were linearly fitted to give a slope corresponding to the waveguide drift. It was attributed to the middle of the time interval concerned. These slope values were plotted versus time and then fitted with a single exponential function

$$\text{slope} = \frac{\delta(d_A')}{\delta t} = ae^{-bt}, \tag{4}$$

which was subsequently integrated to give the part of $d_A'(t)$ due to chip drift. The integration constant was selected to set $d_A = 0$ at that time, when n_F and d_F had been calculated as reference values. This integrated drift curve was then subtracted from the original layer thickness data, d_A', to yield the true thickness of the adlayer, d_A.

Surface plasmon resonance experiments

Surface plasmon resonance experiments were performed with the apparatus described by Terrettaz et al. (1993) using a Kretschmann configuration (Kretschmann, 1972). Thiolipids were immobilized on the gold surface by spontaneous self-assembly from a mixed micelle solution (1 mg/mL lipid in 50 mM OG, dissolved in water, as described elsewhere (Lang et al., 1994)). Incubation times were varied from 2 to 6 h. After washing the thiolipid layer once with 50 mM OG solution and rinsing with water, a second layer was formed on top of it using the same methods as described (see Formation of the lipid bilayer and protein binding).

For some measurements of antibody binding to lipopeptide, the mixed POPC/lipopeptide layer was formed on top of a tetradecanethiol instead of a thiolipid surface. Tetradecanethiol layers were produced by immersion of the gold-covered glass slide in a 1 mg/mL solution of tetradecanethiol in ethanol for 3 h.

Measurements were evaluated as follows. At a fixed refractive index of $n = 1.45$ for the organic layers, Fresnel calculations for our experimental conditions yielded a proportionality constant of 64 Å per degree angle shift in the case of very thin layers ($d_A \ll \lambda$). The observed shifts of the resonance angle were multiplied by this constant to give the mean layer thickness values.

Acknowledgments

We would like to thank the following colleagues from the EPFL for their help: Anne Sévin for providing us with synthesized peptides and antibodies, Tobias Gerfin for performing the ellipsometry measurements, Michael Pawlak for the electrical measurements, Martha Liley and Claus Duschl for critically reading the manuscript. We are grateful to Günther Jung and Karl-Heinz Wiesmüller (University of Tübingen, Germany) for providing us with (NANP)-lipopeptides. This work was supported financially by the Swiss National Science Foundation Priority Program on Biotechnology, projects 5002-35180 (H.V.) and 5002-034779 (H.S.), and by the EUREKA project 2690.1 (H.S., Kommission zur Förderung der wissenschaftlichen Forschung, Bern).

References

Aspnes DE. 1982. Optical properties of thin films. *Thin Solid Films 89*:249–262.

Atherton E, Logan CJ, Sheppard RC. 1979. Peptide synthesis. Part 2. Procedures for solid phase synthesis using *N*α-fluorenylmethoxycarbonyl amino acids on polyamide supports. Synthesis of substance P and of acyl carrier protein 65–74 decapeptide. *J Chem Soc Perkin Trans 1*:538.

Chapman D. 1993. Biomembranes and new hemocompatible materials. *Langmuir 9*:39–45.

Darst SA, Ahlers M, Meller PH, Kubalek EW, Blankenburg R, Ribi HO, Ringsdorf H, Kornberg RD. 1991. Two-dimensional crystals of streptavidin on biotinylated lipid layers and their interactions with biotinylated macromolecules. *Biophys J 59*:387–396.

Duscht, G, Sévin-Landais AF, Vogel H. 1995. Surface engineering: Optimization of antigen presentation in self-assembled monolayers. *Biophys J*, submitted.

Eigen M, Rigler R. 1994. Sorting single molecules: Applications to diagnostics and evolutionary biotechnology. *Proc Natl Acad Sci 91*:5740–5747.

Erdelen C, Häussling L, Naumann R, Ringsdorf H, Wolf H, Yang J, Liley M, Spinke J, Knoll W. 1994. Self-assembled disulfide-functionalized amphiphilic copolymers on gold. *Langmuir 10*:1246–1250.

Feder D, Im MJ, Klein HW, Hekman M, Holzhöfer A, Dees C, Levitzki A, Helmreich EJM, Pfeuffer T. 1986. Reconstitution of β_1-adrenoceptor-dependent adenylate cyclase from purified components. *EMBO J 5*: 1509–1514.

Fenter P, Eberhardt A, Eisenberger P. 1994. Self-assembly of *n*-alkyl thiols as disulfides on Au(111). *Science 266*:1216–1218.

Godson GN. 1985. Molecular approaches to malaria vaccines. *Sci Am* 32–39.

Häussling L, Ringsdorf H, Schmitt FJ, Knoll W. 1991. Biotin-functionalized self-assembled monolayers on gold: Surface plasmon optical studies of specific recognition reactions. *Langmuir 7*:1837–1840.

Heithier H, Fröhlich M, Dees C, Baumann M, Haring M, Gierschik P, Schiltz E, Vaz VL, Hekman M, Helmreich EJ. 1992. Subunit interactions of GTP-binding proteins. *Eur J Biochem 204*:1169–1181.

Hong HG, Jiang M, Sligar SG, Bohn PW. 1994. Cysteine-specific surface tethering of genetically engineered cytochromes for the fabrication of metalloprotein nanostructures. *Langmuir 10*:153–158.

Johnson SJ, Bayerl TM, McDermott DC, Adam GW, Rennie AR, Thomas RK, Sackmann E. 1991. Structure of an adsorbed dimyristoylphosphatidylcholine bilayer measured with specular reflection of neutrons. *Biophys J 59*:289–294.

Kalb E, Frey S, Tamm LK. 1992. Formation of supported planar bilayers by fusion of vesicles to supported phospholipid monolayers. *Biochim Biophys Acta 1103*:307–316.

Kallury KMR, Ghaemmaghami V, Krull UJ, Thompson M. 1989. Immobilization of phospholipids on silicon, platinum, indium/tin oxide and gold surfaces with characterization by X-ray photoelectron spectroscopy and time-of-flight secondary ion mass spectroscopy. *Anal Chim Acta 225*: 369–389.

Kitagawa T, Shimozono T, Aikawa T, Yoshida T, Nishimura H. 1981. Preparation and characterization of hetero-bifunctional crosslinking reagents for protein modifications. *Chem Pharm Bull 29*:1130–1135.

Kogelnik H. 1979. Theory of dielectric waveguides. In: Tamir T, ed. *Integrated optics*. Berlin: Springer Verlag. pp 13–81.

Kooyman RPH, Krull UJ. 1991. Surface plasmon microscopy of two crystalline domains in a lipid monolayer. *Langmuir 7*:1506–1509.

Kretschmann E. 1972. Decay of non radiative surface plasmons into light on rough silver films. *Opt Commun 6*:185–187.

Lang H, Duschl C, Grätzel M, Vogel H. 1992. Self-assembly of thiolipid molecular layers on gold surfaces: Optical and electrochemical characterization. *Thin Solid Films 210/211*:818–821.

Lang H, Duschl C, Vogel H. 1994. A new class of thiolipids for the attachment of lipid bilayers on gold surfaces. *Langmuir 10*:197–210.

Lang H, König B, Vogel H. 1993. Lipid membrane sensors. *European Patent Application No. 93911493.0-2116.*

Lee GU, Chrisey LA, Colton RJ. 1994. Direct measurement of the forces between complementary strands of DNA. *Science 266*:771–773.

McConnell HM, Watts TH, Weis RM, Brian AA. 1986. Supported planar membranes in studies of cell–cell recognition in the immune system. *Biochim Biophys Acta 864*:95–106.

Metzger J, Wiesmüller KH, Schaude R, Bessler WG, Jung G. 1991. Synthesis of novel immunologically active tripalmitoyl-*S*-glycerylcysteinyl lipopeptides as useful intermediates for immunogen preparations. *Int J Pept Protein Res 37*:46–57.

Nellen PM, Lukosz W. 1993. Integrated optical input grating couplers as direct affinity sensors. *Biosensors & Bioelectronics 8*:129–147.

Nie S, Chiu DT, Zare RN. 1994. Probing individual molecules with confocal fluorescence microscopy. *Science 266*:1018–1021.

Pethig R. 1979. *Dielectric and electronic properties of biological materials*. New York: Wiley.

Ramsden JJ, Schneider P. 1993. Membrane insertion and antibody recognition of a glycosylphosphatidylinositol-anchored protein: An optical study. *Biochemistry 32*:523–529.

Ravetch JV, Kinet JP. 1991. Fc receptors. *Annu Rev Immunol 9*:457–492.

Reiter R, Motschmann H, Knoll W. 1993. Ellipsometric characterization of streptavidin binding to biotin-functionalized lipid monolayers at the water/air interface. *Langmuir 9*:2430–2435.

Riddles PW, Blakeley RL, Zerner B. 1983. Reassessment of Ellman's reagent. *Methods Enzymol 91*:49–60.

Romero P, Maryanski JL, Corradin G, Nussenzweig RS, Nussenzweig V, Zavala F. 1989. Cloned cytotoxic T cells recognize an epitope in the circumsporozoite protein and protect against malaria. *Nature 341*:323–326.

Rudy B, Iverson LE, eds. 1992. Ion channels. *Methods Enzymol 207*. London: Academic Press.

Sarin VK, Kent SBH, Tam JP, Merrifield RB. 1981. Quantitative monitoring of solid-phase peptide synthesis by the ninhydrin reaction. *Anal Biochem 117*:147–157.

Schmidt A, Spinke J, Bayerl T, Sackmann E, Knoll W. 1992. Streptavidin binding to biotinylated lipid layers on solid supports. *Biophys J 63*: 1185–1192.

Shinitzky M, ed. 1995. *Biomembranes: Signal transduction across membranes. 3*. Weinheim, FRG: VCH Verlagsgesellschaft mbH.

Spinke J, Liley M, Guder HJ, Angermaier L, Knoll W. 1993. Molecular recognition of self-assembled monolayers: The construction of multicomponent multilayers. *Langmuir 9*:1821–1825.

Spinke J, Yang J, Wolf H, Liley M, Ringsdorf H, Knoll W. 1992. Polymer-supported bilayer on a solid substrate. *Biophys J 63*:1667–1671.

Spohn PK. 1994. Optical restrictions on the quantitative use of grating coupler sensors (GCS). *Sensors and Actuators A 41–42*:516–524.

Stenberg E, Persson B, Roos H, Urbaniczky C. 1991. Quantitative determination of surface concentration of protein with surface plasmon resonance using radiolabeled proteins. *J Colloid Interface Sci 143*:513–526.

Strader CD. 1994. Structure and function of G-protein-coupled receptors. *Annu Rev Biochem 63*:101–132.

Swalen JD. 1986. Optical properties of Langmuir–Blodgett films. *J Mol Elec 2*:155–181.

Terrettaz S, Stora T, Duschl C, Vogel H. 1993. Protein binding to supported lipid membranes: Investigation of the cholera toxin-ganglioside interaction by simultaneous impedance spectroscopy and surface plasmon resonance. *Langmuir 9*:1361–1369.

Thompson NL, Poglitsch CL, Timbs MM, Pisarchick ML. 1993. Dynamics of antibodies on planar model membranes. *Acc Chem Res 26*:567–573.

Tiefenthaler K, Lukosz W. 1989. Sensitivity of grating couplers as integrated-optical chemical sensors. *J Opt Soc Am B 6*:209–219.

Ulman A. 1991. *An introduction to ultrathin organic films: From Langmuir–Blodgett to self-assembly*. San Diego, California: Academic Press.

Unwin N. 1993. Neurotransmitter action: Opening of ligand-gated ion channels. *Cell 72*:31–41.

Vandenberg ET, Bertilsson L, Liedberg B, Udval K, Erlandsson R, Elwing H, Lundström I. 1991. Structure of 3-aminopropyl-triethoxysilane on silicon oxide. *J Colloid Interface Sci 147*:103–118.

Weber PC, Ohlendorf DH, Wendoloski JJ, Salemme FR. 1989. Structural origins of high-affinity biotin binding of streptavidin. *Science 243*:85–88.

Wiener MC, White SH. 1992. Structure of a fluid dioleoylphosphatidylcholine bilayer determined by joint refinement of X-ray and neutron diffraction data. *Biophys J 61*:434–447.

Wise DL, Wingard LB, eds. 1991. *Biosensors with fiberoptics. Contemporary instrumentation and analysis*. New Jersey: Humana Press.

Zhou Y, Laybourn PJR, Magill JV, De La Rue RM. 1991. An evanescent fluorescence biosensor using ion-exchanged buried waveguides and the enhancement of peak fluorescence. *Biosensors & Bioelectronics 6*:595–607.